Integrative Biology

RSC Publishing

PAPER

View Article Online
View Journal | View Issue

Cite this: *Integr. Biol.*, 2013, **5**, 1282

ERG9 and *COQ1* disruption reveals isoprenoids biosynthesis is closely related to mitochondrial function in *Saccharomyces cerevisiae*

Beibei Huang,[ab] Jing Guo,[a] Lianna Sun[c] and Wansheng Chen*[a]

Received 2nd April 2013,
Accepted 5th August 2013

DOI: 10.1039/c3ib40063h

www.rsc.org/ibiology

Understanding *in vivo* regulation of isoprenoid biosynthesis is important for identifying strategies to improve carbon fluxes to desirable endproducts. To study the relevance of gene functions, substrate availability, metabolic flux, and the energetics of resource utilization for isoprenoids biosynthesis, *Saccharomyces cerevisiae* was co-engineered with endogenous deregulated *erg9* and/or *coq1* and exogenous plant genes that will lead to sesqui- and diterpene production. The flow of substrates through the MVA pathway statistically showed isoprenoids precursor levels were tightly regulated by *erg9* and *coq1* genes in *S. cerevisiae*. Physiological analysis by fluorescent probes and labeling techniques revealed elimination of the competing and/or degrading pathways by gene knockout can increase cellular stresses and change the energy metabolism. To further evaluate the role of *erg9* and *coq1* in the regulation of isoprenoids synthesis, heterologous terpene synthases from plants were introduced into *S. cerevisiae*, including the wild-type and mutant strains along with feeding of various metal cofactors under anoxic/oxic conditions. The product distribution in the strains indicated that the energy barrier could be the reason that different metal ion-assisted electrophilic attacks initiated carbocation formation, carbocation stabilization, and rearrangement, incorporating exquisite regio- and stereospecificity, to generate structurally diverse products. The yeast altered in the profile of terpenoids and their precursor pools aided the mechanisms of terpenoid biosynthesis and its regulation, highlighting the need for mitochondrial function when engineering metabolic flux using assumptions based on a comprehensive network of the mitochondrial system.

Insight, innovation, integration

Systems metabolic engineering, which incorporates the concepts and techniques of systems biology, synthetic biology *etc.* at the systems level, is changing the way microbial cell factories are designed and optimized. We constructed a series of *Saccharomyces cerevisiae* mutants using gene disruption, then adopted GC/MS, fluorescent probes and labeling techniques to measure flux flow as well as global cellular energy status in response to these gene disruptions. Furthermore, we continued our study by expression of terpene synthases and observing the product distribution produced in the strains under different metabolic backgrounds. This work highlights the functional interrelationships between mitochondria and isoprenoid biosynthesis, which suggests the activation of mitochondria energy metabolism could drive terpenoid biosynthesis in microorganisms at more advanced levels.

1. Introduction

Synthetic biology and metabolic engineering of microorganisms through the expression of one or more plant genes, often in combination with genetic alteration of the host cell metabolism, has become an increasingly important route for small molecule synthesis. One group of compounds that has particularly benefited from this approach is the isoprenoids (sometimes referred to as terpenoids). Terpenoids represent one of the largest classes of secondary metabolites that include pharmaceuticals, cosmetics, and potential biofuels candidates.[1–4] However, supply limitations prevent the large scale use of some molecules. It is therefore often advantageous to transfer pathways from the original producer to a dedicated cell factory, such as the yeast *Saccharomyces cerevisiae*.

[a] *Department of Pharmacy, Changzheng Hospital, Second Military Medical University, Shanghai 200003, China. E-mail: chenwanshengsmmu@aliyun.com, chenws@vnet.citiz.net; Fax: +86-21-81871314; Tel: +86-21-81871347*

[b] *California Institute for Quantitative Biosciences, University of California, Berkeley, CA 94720, USA*

[c] *Department of Pharmacognosy, School of Pharmacy, Second Military Medical University, Shanghai 200433, China*

Yeast has a high inherent capacity for the biosynthesis of isoprenoid precursors that may be directed to the production of heterologous compounds. The MVA pathway is the only pathway involved in the biosynthesis of isoprenoid precursors in *S. cerevisiae*. The MVA pathway can be considered to consist of two distinct parts: an early isoprenoid section of the pathway, common to many branches and ending with the formation of hexaprenyl diphosphate (HPP), and a late part of the pathway mainly dedicated to ergosterol biosynthesis in *S. cerevisiae* (Fig. 1). Isoprenoid accumulation seems to be tightly regulated by certain genes within this metabolic pathway, but the detailed regulatory mechanism remains unknown. Two distinct but interconnected major sites of regulation are investigated: one is *erg9* gene competing for FPP through conversion of FPP to squalene, the other is *coq1* gene which lies in the downstream pathway of geranyl diphosphate (GPP, the C10 precursor to monoterpenes), farnesyl diphosphate (FPP, the C15 precursor to sesquiterpenes and triterpenes) and geranylgeranyl diphosphate (GGPP, the C20 precursor to diterpenes) (Fig. 1).

In many other cases of metabolic engineering, controlling the degradation or catabolism of the targeted products is very important. There are numerous successful examples of this popular approach, however, several reasons argue against the efficiency for this means in terpenoid engineering: one, in *S. cerevisiae*, *erg9* and *coq1* are vital for yeast growth. Gene disruption may also significantly bring about deleterious effects on the engineered cell's metabolism, thus weakening the efficient formation of targeted compounds. To tackle more difficult problems that result from the complex nature of metabolic and cellular regulatory networks, a greater understanding of biological information related to the MVA pathway is necessary.

To this end, synthetic biologists and metabolic engineers utilize a variety of analytical methods to quantitatively understand and modulate metabolism, with an emphasis on the global state of the cell, and not on individual reactions.[5] This represents a paradigm shift from focusing only on the product forming step, and instead understanding the pathway in the

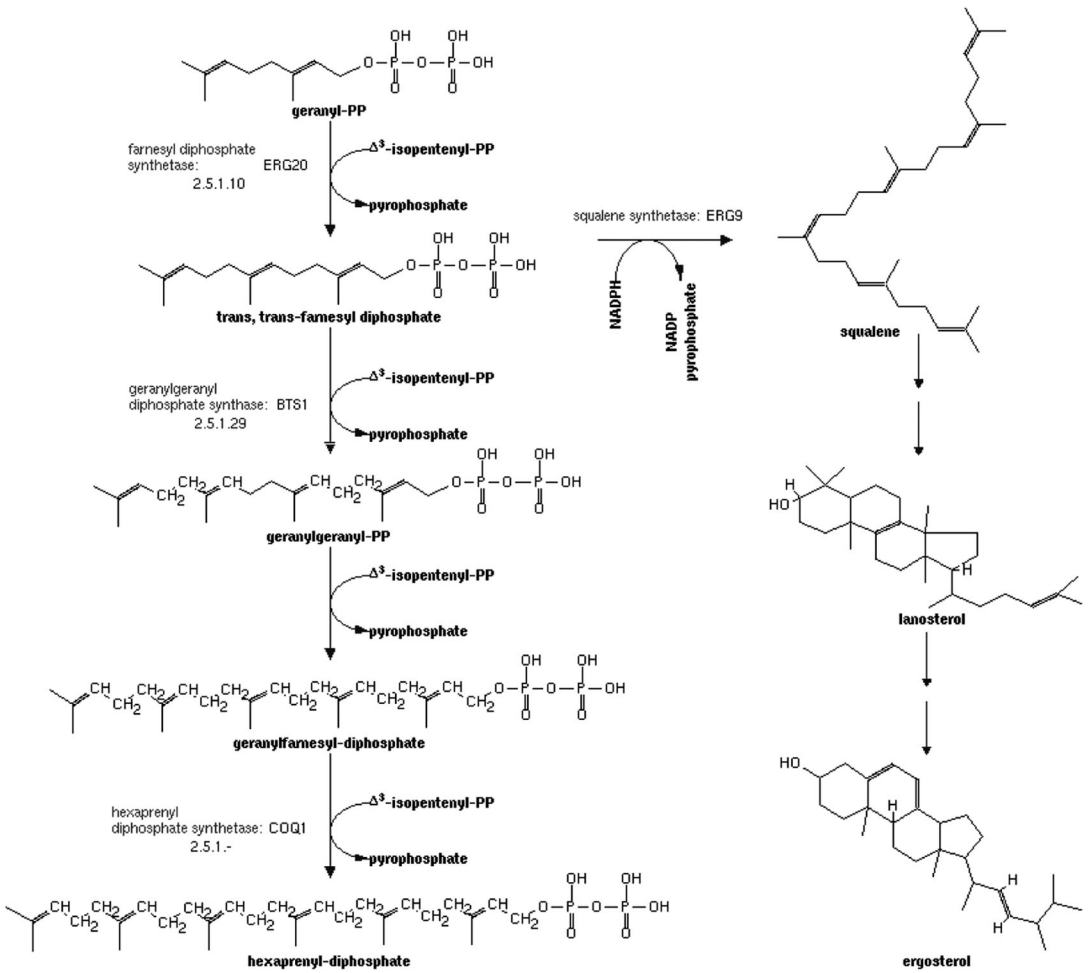

Fig. 1 Biosynthetic routes to polyprenyl pyrophosphates isoprenoid biosynthetic pathways of *S. cerevisiae*. The different classes of isoprenoids precursors, isopentenyl-PP: isopentenyl diphosphate, IPP; geranyl-PP: geranyl diphosphate, GPP; *trans*,*trans*-farnesyl diphosphate: farnesyl diphosphate, FPP; geranylgeranyl-PP: geranylgeranyl diphosphate, GGPP; geranylfarnesyl diphosphate: GFPP; NADPH: reduced form of nicotinamide-adenine dinucleotide phosphate; NADP: nicotinamide adenine dinucleotide phosphate. The indicated enzymes are: (1) farnesyl diphosphate synthase (FPPS) ERG20 EC: 2.5.1.10; (2) geranylgeranyl diphosphate synthase (GGPPS) BST1 EC:2.5.1.29; (3), hexaprenyl diphosphate synthase (HPPS) COQ1 EC:2.5.1.-; (4) squalene synthase (ERG9).

context of the entire cell. Advances in other complementary biological disciplines, specifically 'omics' technologies,[6,7] computational systems biology,[8,9] protein engineering[10,11] and synthetic biology[12–16] stand to contribute greatly to our ability to engineer the cell by improving the means to identify and make perturbations at will.

The physiological features (such as cellular stresses and energy status) and molecular pathway analyses (such as intermediate quantification) of these mutants and the parental strains has not been reported. It will also be interesting to see if the elevating metabolic flux in MVA pathway, more nutrients cofactors, and anoxic conditions improve diversity and yield of products obtained from heterologous terpenoid pathways.

In this study, we have first controlled *erg9* and *coq1* expressions by one deletion allele of corresponding genes in *S. cerevisiae*. Secondly, the mutants and the parental strain were subsequently characterized in terms of abundance of metabolic intermediates in the isoprenoid biosynthetic pathways by gas chromatography-selected ion-monitoring mass spectrometry (GC-SIM-MS) for identifying gene effects on metabolic flux in isoprenoid pathway. Next, the measurements of energy-dependent efflux activity of membrane transporters, intracellular ATP concentration, mitochondrial membrane potential, and endogenous reactive oxygen species (ROS) generation were carried out by the application of fluorescence and chemiluminescence analysis, showing that a physiological metabolism shift occurred in response to gene disruption. Furthermore, we observed the distribution of sesqui- and diterpenes from FPP or GGPP by introduction of terpene synthases into the strains along with feeding of various metal cofactors in the presence or absence of oxygen: one β-cubebene synthase from *Magnolia grandiflora*[17] for sesquiterpene production, and copalyl diphosphate synthases (CPS) combined with kaurene synthase-like (KSL) from *Salvia miltiorrhiza* Bunge for diterpene production.[18] Our present ability to investigate secondary metabolism from a combined biochemical, molecular, cellular, and physiological perspective has improved our appreciation for the complex biology of terpenoid pathways. This work also highlights the functional interrelationships between mitochondria and isoprenoid biosynthesis, which suggests the activation of mitochondria energy metabolism could be good for terpenoid metabolic engineering in microorganisms at more advanced levels.

2. Materials and methods

2.1. Chemicals and plant material

All standards were purchased from Sigma-Aldrich, Steinheim, Germany. Bacterial alkaline phosphatase was from TaKaRa, Japan. Pyrophosphatase from *S. cerevisiae* was obtained from Sigma-Aldrich. All solvents were of analytical grade or higher quality. Other reagents were from Sigma-Aldrich. Plant leaves were collected from *M. grandiflora* grown on the campus of Second Military Medical University. The *S. miltiorrhiza* hairy root cultures were obtained by infecting sterile plantlets (collected from ShangLuo Shanxi province, PRC) with a Ri T-DNA bearing *Agrobacterium rhizogenes bacterium* (C58C1).

2.2. Yeast strains, culture media and conditions

All the recombinant strains were generated from the BY4743 *S. cerevisiae* wild-type strain (Invitrogen, USA) (see Table 1). Yeast extract peptone dextrose (YPD), synthetic dextrose (SD), synthetic galactose (SG) and 5-fluoro-orotic acid (5-FOA) plates were prepared as previously described.[19–21] Solid media contained, in addition, 2% agar (Difco Laboratories). YPD medium was comprised of 10 g L^{-1} yeast extract, 20 g L^{-1} peptone, and 20 g L^{-1} glucose. SD medium was comprised of 20 g L^{-1} glucose, 6.7 g L^{-1} yeast nitrogen base without amino acids (Difco/BD Diagnostic Systems, USA), and 0.77 g L^{-1} complete supplement mixture lacking specified amino acid(s) for auxotrophic marker(s) (Clontech Laboratories, USA), pH 6.0. SG medium was comprised of 20 g L^{-1} galactose, 6.7 g L^{-1} yeast nitrogen base without amino acids, and 0.77 g L^{-1} complete supplement mixture lacking specified amino acid(s) for auxotrophic marker(s), pH 6.0. 5-FOA plates were comprised of 20 g L^{-1} glucose, 6.7 g L^{-1} yeast nitrogen base without amino acids,

Table 1 Yeast strains and plasmids used in this study

Strain	Genotype	Origin
BY4743	*MAT a/α, his3Δ1/his3Δ1, leu2Δ0/leu2Δ0, met15Δ0/MET15, LYS2/lys2Δ0, ura3Δ0/ura3Δ0*	Euroscarf accession no. Y20000
BY4743-Δ*ERG9*	*Mat a/α, his3Δ1/his3Δ1, leu2Δ0/leu2Δ0, met15Δ0/MET15, LYS2/lys2Δ0, ura3Δ0/ura3Δ0, ERG9::kanMX4/ERG9*	This study
BY4743-Δ*COQ1*	*Mat a/α, his3Δ1/his3Δ1, leu2Δ0/leu2Δ0, met15Δ0/MET15, LYS2/lys2Δ0, ura3Δ0/ura3Δ0, COQ1Δ0/COQ1*	This study
BY4743-Δ*ERG9*-Δ*COQ1*	*Mat a/α, his3Δ1/his3Δ1, leu2Δ0/leu2Δ0, met15Δ0/MET15, LYS2/lys2Δ0, ura3Δ0/ura3Δ0, ERG9::kanMX4/ERG9, COQ1Δ0/COQ1*	This study
Plasmids		
pUG6	The loxP-kanMX-loxP disruption module	Euroscarf accession no. P30114
pUG72	The loxP-*URA3*-loxP disruption module	Euroscarf accession no. P30117
pESC-Ura	2μ *URA3 GAL1* and *GAL10* promoters, binary vector	Stratagene
pYES2	2μ *URA3 GAL1* promoter	Invitrogen
pESC-SmKSL-SmCPS	The kaurene synthase-like and the copalyl diphosphate synthase in pESC-Ura	This study
pYES-Mg25	β-Cubebene synthase in pYES2	This study

0.77 g L^{-1} complete supplement mixture lacking uracil, 100 mg L^{-1} uracil, 1 g L^{-1} 5-FOA (Zymo Research, USA), and 20 g L^{-1} agar. Yeast transformants containing the G418 (kanMX) were selected on YPD supplemented with 200 μg mL^{-1} geneticin (Life Technologies). Selection for the *URA3* cassette was performed on SD-Ura medium. For induction of genes expressed from the *GAL1* promoter, *S. cerevisiae* strains were grown in SG dropout media. Ura^- cells were selected on synthetic complete medium containing 5-FOA at 1 mg mL^{-1}.[22] Different metal ion medium was comprised of SD medium with 3.1 g L^{-1} K_2HPO_4, 2.5 g L^{-1} $MgSO_4$, 1.55 mg L^{-1} $MnCl_2{\cdot}2H_2O$, or 6 mg L^{-1} $FeSO_4{\cdot}7H_2O$ respectively. All strains were grown in shake flasks at 30 °C and 200 rpm and the ratio of flask volume : medium was 5 : 1.

2.3. Yeast strains development

One allele deletion of the *erg9* or *coq1* ORF was accomplished with a PCR-mediated gene disruption. We pooled two preparative PCR reactions for a gene disruption. Firstly, we amplified two cassettes for the different gene disruption experiments with the following primers: ERG9.F and ERG9.R for disruption of *ERG9*, COQ1.F and COQ1.R for that of *COQ1* (Table 2). The gene disruption cassette consists of a selection marker gene marker, usually conferring drug resistance or prototrophy, flanked by two 34 bp *loxP* sequences as direct repeats located adjacent to 45 bp of sequence flanking the chromosomal target sequence (ORF) to be deleted. Each chimeric primer consists of 45 nucleotides homologous to the appropriate flanking region of the genomic target locus and about 20 nucleotides, which allow for amplification of the *kanMX4* or *URA3* cassette. Plasmid pUG6 was used as the PCR template to generate the *loxP–kanMX4–loxP* disruption cassette, and PUG72 used for the *loxP–URA3–loxP* disruption cassette. The PCR procedure was conducted under the following conditions: 5 min at 94 °C, 30 cycles (40 s at 94 °C, 1 min at 58 °C, 2 min at 72 °C) and 7 min at 72 °C. The PCR product was purified and the cassettes used for yeast transformation. Lithium acetate transformations were performed by standard methods.[23]

After transformation of the linear disruption cassette into yeast cells, selected transformants were checked by PCR for correct integration of the cassette and concurrent deletion of the chromosomal target sequence. Correct targeting of the *kanMX4* or *URA3* module into the genomic locus was verified with genomic DNA. The verification PCRs were done using combinations of primers complementary to sequences within the cassette and to sequences within or flanking the target sequence (Table 2). Wild-type (WT) *S. cerevisiae* colonies were tested in parallel as a negative control. The PCR reaction was as described for the generation of the disruption cassette. The conditions were: 5 min at 94 °C, 30 cycles (40 s at 94 °C, 1 min at 58 °C, 2 min at 72 °C) and 7 min at 72 °C. About 15 μL of the PCR reaction were loaded on an agarose gel.

One allele of *erg9* was removed from the BY4743 strain; the resulting strain harbored mutations in *erg9* gene and was named BY4743-Δ*ERG9*. After initial selection on SD-Ura plates, transformants harbored mutations in *coq1* gene were cultured and plated on 5-FOA plates as a selection for the loss of the *URA3* marker; the resulting strain was named BY4743-Δ*COQ1*. In order to obtain *erg9*/*coq1* dual disruptants, the BY4743-Δ*ERG9* strain was chosen for further disruption of *coq1*. It was also transformed with the *loxP–URA3–loxP* disruption cassette, followed by selection on SD-Ura plates with G418. Subsequently, cells that lost *URA3* due to recombination between the flanking repeats were selected on 5-FOA plates, resulting in BY4743-Δ*ERG9*-Δ*COQ1*. Excision of *URA3* was confirmed based on the PCR product obtained with primers Ura3 F and Ura3 R (a 1 kb product for strains with the integrated *URA3* cassette, and no product for strains that subsequently lost the *URA3* cassette).

2.4. Construction of plasmids

All molecular manipulations were performed according to standard methodologies described in ref. 24. The Mg25 (β-cubebene synthase) (GenBank accession EU366429) was isolated using an RT-PCR strategy and mRNA isolated from *M. grandiflora* leaves as described by Lee and Chappell (2008),[17] and the SmCPS (accession EU003997), and SmKSL (accession EF635966) genes were isolated by RT-PCR from *S. miltiorrhiza* hairy roots according to the information provided by Gao *et al.* (2009).[18] The amplified PCR product was purified and cloned into PMD18-T vector and then was verified by complete sequencing.

Table 2 Primers used in this work. Lower case letters indicate nucleotides homologous to sequences left and right of the cloned disruption cassettes

Primers	Sequence	Target gene/disruption marker
Gene disruption		
ERG9.F	5′-AGAAGCGGAAAACGTATACACGTCACATATCACACACACACAATGcagctgaagcttcgtacgc-3′	*erg9*, kanMX
ERG9.R	5′-TTATTGTTCGGAGTTGTTTGTTTATGTTATTTGGCGCAGACTTCAgcataggccactagtggatctg-3′	*erg9*, kanMX
COQ1.F	5′-CAAGAAGTGTGCCATTCAGTCCGAATTGAGTACAGTGGGACGATGtcgttttatttaggttctatcgagg-3′	*coq1*, *URA3*
COQ1.R	5′-ATTTTCTCTTTATTCTTCACCCTTTATTTGAAATTTCAAGGTTTAgagatcccaatacaacagatcacg-3′	*coq1*, *URA3*
Verification		
ERG9A	5′-CTCAGTACATTTCATAGCCCATCTT-3′	*erg9*
Kan-B	5′-GGATGTATGGGCTAAATG-3′	
COQ1A	5′-ATCTCTTTCTTTCTAGCGAATCTCC-3′	*coq1*
Ura-B2	5′-TCCAATGCAGACCGATCTTCTACCC-3′	
Ura3 F	5′ -ATGTCCACAAAATCATATACCAGTAGA-3′	*Ura3*
Ura3 R	5′-CTTCCCATCCAGCATTTCTGTATCT-3′	

Yeast expression vector pESC-Ura was obtained from Stratagene (La Jolla, CA), and pYES2 vector was from Invitrogen (Carlsbad, CA). For Mg25, the forward primer 5′-GGGGTACCATGGATAGTCCCACTACTCAAAGGC-3′ and the reverse primer 5′-ATTTGCGGCCGCTTAAAGTGGAATAGGGTCCACAAAC-3′ were used to amplify the ORF gene, then the resulting amplicon was digested with KpnI/NotI, and transferred into pYES2 to yield sequence verified pYES-Mg25. For SmKSL, after the forward primer 5′-TTGGATCCATGTCGCTCGCCTTCAACCCG-3′ and the reverse primer 5′-TTGTCGACTTTCCCTCTCACATTATTAGC-3′ were used to amplify the coding region of SmKSL, the amplicon was incompletely digested with BamHI/SalI, and transferred into pESC-Ura to yield pESC-SmKSL, which would be used as the parent plasmid for coexpression with the SmCPS as described below. For SmCPS, the forward primer 5′-TTGCGGCCGCATGGCCTCCTTATCCTCTACA-3′ and the reverse primer 5′-GGACTAGTCGCGACTGGCTCGAAAAG-3′ were used to amplify the full coding region of SmCPS, the resulting PCR fragment was digested with NotI/SpeI and transferred into pESC-SmKSL (see above) to yield sequence verified pESC-SmKSL-SmCPS that contained the kaurene synthase-like (under GAL1 control) and the copalyl diphosphate synthase (under GAL10 control).

2.5. Yeast expression

Four types of yeast strains (wild type, *coq1* disruption, *erg9* disruption, *coq1* and *erg9* dual disruption) were transformed with the respective vector constructs using the Yeast Transformation System 2 from Clontech (Palo Alto, CA), followed by selection for prototrophic growth on minimal media without supplementation for the appropriate metabolite. The expression protocol was essentially that from the pYES2 Instruction Manual (Invitrogen). Transformed yeast cells were selected on plates of SD dropout medium, and colonies were used to inoculate liquid SD dropout medium for overnight culture at 30 °C. After collection by centrifugation, the cells were suspended in 100 mL of SG dropout medium to $A600 \approx 0.4$ and cultured at 30 °C in 250 mL Erlenmeyer flasks with vigorous shaking (200 rpm) for up to 3 days ($A600 > 2.0$) after induction with 2% galactose. An equal volume of dichloromethane was vigorously mixed with an aliquot of cell culture, then incubated at room temperature for another 20 min, and the phases separated by brief centrifugation in a clinical centrifuge. The dichloromethane extract was ready to be analyzed directly by GC-MS, or in some cases concentrated under a N_2 stream before analysis.

2.6. Metabolite analyses

Aliquots of the various samples were analyzed for terpene constituents with a Thermo Scientific TRACE GC Ultra™ equipped with a Thermo Scientific DSQ™ II single quadrupole mass spectrometer and a HP-5MS capillary column (30 m × 0.25 mm i.d., 0.25 μm film thickness). ToxLab™ 2.0 software automated the acquisition and processing of all data, including quantification and ion ratio confirmation calculations. All compounds detected were confirmed by comparing retention time and mass spectra with authentic standards, or by comparison with mass spectra reported in the NIST mass spectra library version 2.0 and MassFinder 2.3 software.

Identification of terpenes in the plants was performed by extracting volatile compounds from the head-space of the samples on 100 μm polydimethyl siloxane (PDMS) fibers (Supelco, Bellefonte, PA, USA). Fibers were conditioned according to the suppliers' instruction. 2 g of young *Magnolia* leaf tissue or fresh *Salvia* hairy root sample was first pulverized in liquid nitrogen with a mortar and pestle, and then stored in 4 mL screw cap glass vials at −20 °C until analysis. The contents of vials were thawed on ice and allowed to equilibrate at room temperature. Extraction was performed for 25 min at 60 °C while mixing the sample with a small magnet. After extraction the analytes were thermally desorbed at 250 °C from the solid phase microextraction (SPME) fiber into the injector of the gas chromatogram in the splitless mode. The oven temperature was held initially at 60 °C for 2 min, and then raised to 300 °C by a ramp of 20 °C min^{-1}. The oven temperature was maintained at this temperature for 5 min to equilibrate.

To analyse the intermediates involved in the isoprenoid pathway in the mutant yeast strains, 100 mL of SD medium (not any specified amino acid dropout) were centrifuged at 4 °C for 10 min at 3500 × *g* and the cell pellets were washed twice with PBS solution, after culturing at 30 °C, 200 rpm for 48 h. The cells were then suspended in a 2 mL buffer (1 M diethanolamine, 0.5 mM $MgCl_2$, pH 9.8) and vortexed for 1 min. After cell lysis by sonication for 20 min, the suspension was vortexed for 1 min, followed by the addition of pyrophosphatase (3 U) shaken for 60 min at 70 °C. Subsequently, alkaline phosphatase (3 U) was added to the sample obtained above, incubated at 65 °C for 45 min and extracted with 1 mL hexane. Glass vials with Teflon-lined caps were used for hexane extractions. The mixture was vortexed for 3 min and centrifuged at 12 000 × *g* for 20 min. The hexane phase was decanted and used for GC-MS analysis. The initial oven temperature was 100 °C, both detector and injector temperatures were 270 °C. To determine the conversion rate for GPP, FPP and GGPP to the corresponding alcohols, the column oven temperature was programmed to rise from an initial temperature of 100 °C (5 min) to 250 °C at 10 °C min^{-1}, and was held at 250 °C for 5 min. To quantify target metabolites, after 2 min the initial oven temperature of 100 °C was increased to 300 °C at a rate of 10 °C min^{-1} and held for 15 min at this temperature. The ion source temperature was 250 °C. Mass spectra were recorded at 70 eV, scanning from 10 to 650 atomic mass units, and compared to authentic standards (retention times and mass spectra) for verification. The DSQ II was operated in selected ion monitoring mode (SIM), collecting 2 ions each, as representative ions of target compounds. Quantification masses *m*/*z*—GOH (69, 93), FOH (69, 93), GGOH (69, 93), squalene (69, 81), ergosterol (363, 396), and lanosterol (411, 426).

For terpene analyses in the yeast strains transformed with heterologous terpene synthases, both detector and injector ports were maintained at 250 °C in the splitless mode and the initial oven temperature of 60 °C (2 min) was increased in a 20 °C min^{-1} gradient to 300 °C, and held at 300 °C for 5 min.

The ion source temperature was 250 °C. Mass spectra were recorded at 70 eV and scanned from 41 to 450 atomic mass units.

2.7. Glucose-induced R6G efflux assay

The glucose-induced efflux of R6G (Sigma) from *S. cerevisiae* strains was investigated. Cells in the middle logarithmic phase were collected by centrifugation at 3000*g* for 5 min and washed three times with phosphate buffered saline (PBS; 10 mM phosphate buffer, 2.7 mM potassium chloride, 140 mM sodium chloride, pH 7.4) buffer. Then cells were resuspended at a concentration of 1×10^7 cells per mL in PBS buffer containing 5 mM 2-deoxy-D-glucose and 10 μM R6G. Cell suspensions were incubated at 30 °C with shaking (200 rpm) for 90 min to allow R6G accumulation under glucose starvation conditions. The starved cells were washed twice in PBS buffer, and 1 mL portions were incubated at 30 °C for 5 min before the addition of 1 mM glucose to initiate R6G efflux. At specified intervals after the addition of glucose, the cells were removed by centrifugation. Triplicate 100 μL volumes of the cell supernatants were transferred to 96-well flat-bottom microtiter plates on a Polarstar Optima instrument (BMG Labtech, Offenburg, Germany). The fluorescence of the samples was measured with an excitation wavelength at 515 nm and an emission wavelength at 555 nm.

2.8. Measurement of intracellular ATP levels, mitochondrial membrane potential and ROS levels

The mutant and the parental wild-type *S. cerevisiae* strains in middle logarithmic phase were adjusted to 1×10^8 cells per mL and serial 10-fold dilutions with YPD broth. A total of 100 μL from the cell suspensions and a same volume BacTiter-Glo reagent (Promega Corporation, Madison, WI) were mixed completely and incubated for 10 min at room temperature. Then the luminescent signals were determined on a TD 20/20 luminometer (Turner Biosystem, Sunnyvale, CA) with an integration time of 1 s per sample. The control tube without strains was to obtain a value for background luminescence. The signal-to-noise ratio was calculated: S/N [mean of signal − mean of background]/standard deviation of background. A standard curve for ATP increments (from 1 μM to 10 pM) was constructed. Signals represented the mean of three separate experiments, and the ATP content was calculated from the standard curve.

Cultured cells were collected by centrifugation, washed and adjusted to 1×10^6 cells per mL with PBS buffer. After treatment with 10 μg mL^{-1} of 5,5′,6,6′-tetrachloro-1,1′,3,3′-tetraethylbenzimidazolcarbocyanine iodide[25] (JC-1; Molecular Probes, Inc., Eugene, OR) at 30 °C for 15 min, cells were washed twice with PBS buffer and analyzed on a POLARstar Galaxy (BMG, Labtech, Offenburg, Germany) at 485 nm excitation wavelength and emission wavelength shifting from green (~525 nm) to red (~590 nm). Mitochondrial membrane potential was determined by the ratio of red to green fluorescence intensity (FI).

Intracellular levels of ROS were measured with 2,7-dichlorofluorescein diacetate (DCFH-DA, Molecular Probes, USA). Briefly, cultured cells were collected by centrifugation and washed three times with PBS. Subsequently, the cells were adjusted to 3×10^7 cells per mL. After being incubated with 20 μg mL^{-1} of DCFH-DA for 30 min at 30 °C and 200 rpm, the cells were washed three times and resuspended in PBS buffer. Control groups were treated with PBS. FI values were detected on the POLARstar Galaxy with excitation wavelength at 488 nm and emission wavelength at 525 nm. The kinetic measurements of ROS were continued for 48 h after the treatments. ROS production was calculated by subtracting the FI value of cells treated with PBS alone from that of cells treated with DCFH-DA.

3. Result

3.1. A series of mutants and recombinants construction

FPP is at a metabolic branching point in the terpenoid pathway in yeast (Fig. 1) and several enzymes, located in different cellular compartments, can compete for it.[26] HPP synthase, encoded in *S. cerevisiae* by *COQ1/YBR003W*, utilizes GGPP as part of the ubiquinone biosynthesis pathway and the protein geranylgeranylation process. To evaluate whether these reactions can affect metabolic flux toward sesqui- and diterpenes production, we developed a series of *Saccharomyces cerevisiae* mutants (BY4743-Δ*ERG9*, BY4743-Δ*COQ1*, BY4743-Δ*ERG9*-Δ*COQ1*c), and constructed two yeast plasmids containing sesqui- or diterpene synthase, respectively. The mutants and the parental strains were further engineered to express one or more of the heterologous terpenoid pathway enzymes from *M. grandiflora* and *S. miltiorrhiza*. The resulting engineered yeast strains were grown in the presence of galactose and assayed for the expected products.

3.2. Effect of *erg9* and *coq1* disruption on the flow of substrates through the MVA pathway

By utilizing the established method,[27] we compared metabolic changes in MVA pathway in the yeast mutants with those in parental strains. Synchronized yeasts at 0 h continued to grow and reach the metabolic steady state after 48 h. Six major metabolites were quantified by GC-MS (Table 3). To enhance substrate availability for foreign terpenoid production *via* elimination of competing and/or degrading pathways, we deleted one allele of *erg9* and/or *coq1* by gene disruption. The absolute flux towards ergosterol, when normalized to OD600 units, in *erg9*Δ/*coq1*Δ as well as in a wild type background was similar to that calculated per total culture; the maximized concentrations of terpenoid precursors were observed compared to that in the WT, *erg9*Δ and *coq1*Δ background. The ergosterol flux in *erg9*Δ mutant has decreased relative to the others in an absolute sense.

3.3. *Erg9* and *coq1* disruption significantly changed global cellular energy status

In the present study, the wild-type strain and mutant strains were physiologically characterized to investigate the overall

Table 3 Normalized concentrations of GPP, FPP, GGPP, squalene, ergosterol and lanosterol to OD_{600} in 48 h

Type	GPP (nM/OD_{600})	FPP	GGPP	Squalene	Ergosterol	Lanosterol	Absolute flux towards ergosterol
Wild type (mean ± SD, n = 6)	0.045 ± 0.003	0.087 ± 0.006	0.041 ± 0.003	0.239 ± 0.015	0.287 ± 0.010	0.080 ± 0.002	0.605
RSD (%)	6.93	7.22	8.12	6.31	3.65	2.19	
ERG9 disruption (mean ± SD, n = 6)	0.078 ± 0.004	0.096 ± 0.012	0.061 ± 0.004	0.121 ± 0.015	0.194 ± 0.013	0.054 ± 0.001	0.369
RSD (%)	4.85	12.18	6.64	12.32	6.57	1.78	
COQ1 disruption (mean ± SD, n = 6)	0.044 ± 0.003	0.056 ± 0.003	0.034 ± 0.002	0.548 ± 0.030	0.423 ± 0.019	0.099 ± 0.002	1.070
RSD (%)	6.43	6.12	5.06	5.45	4.43	1.82	
ERG9 and COQ1 disruption (mean ± SD, n = 6)	0.083 ± 0.004	0.211 ± 0.011	0.113 ± 0.004	0.281 ± 0.025	0.226 ± 0.017	0.056 ± 0.003	0.563
RSD (%)	4.90	5.11	3.52	8.87	7.46	4.93	

cellular performance of these strains in response to genetic modification. *Erg9* encodes farnesyl-diphosphate farnesyl transferase (also called squalene synthase), an enzyme that is crucial for balancing the incorporation of farnesyl diphosphate (FPP) into sterol and nonsterol isoprene synthesis. *Coq1*, belonging to mitochondrial enzymes, has been shown to be required for Q biosynthesis and function in respiration. Because *coq1* and *erg9* contribute many different functions to cellular physiology, it is of interest to ask what kinds of changes might be tolerated by cells without affecting this fundamental physiological role. Cellular stress response, transporter system, energy generation and so on were investigated.

Glucose-induced R6G efflux clearly shows *coq1* disruptant effluxed the most R6G in four types of yeast strains in the presence of glucose, while *coq1* and *erg9* dual disruptant effluxed the least R6G. For the efflux from deenergized (by incubation with 2-deoxy-D-glucose), there was no significant difference between strains, but it could be observed that R6G efflux from the *erg9* and *coq1* dual disruptant was lowest. Within 10 min of adding glucose, the extracellular R6G concentration of all strains had greatly increased. R6G efflux from wild type, *coq1* disruptant, *erg9* disruptant, *erg9* and *coq1* dual disruptant in the presence of glucose was 2.27, 3.64, 2.89, 2.31-fold greater than that in the absence of glucose respectively (Fig. 2).

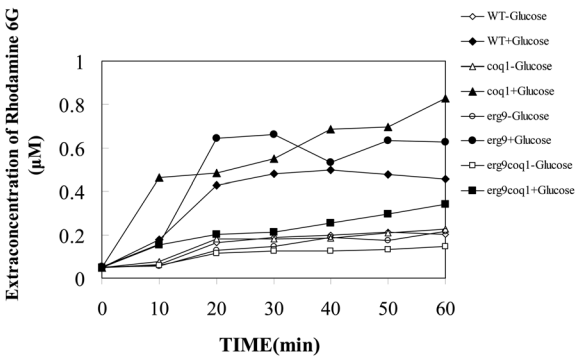

Fig. 2 Energy-dependent efflux of rhodamine 6G in *S. cerevisiae*. Each sample was assayed in triplicate. ''−'' and ''+'' signals means absence and presence of glucose (WT, wild type; coq1, *coq1* disruption; erg9, *erg9* disruption; erg9 Coq1, *coq1* and *erg9* disruption).

Since changes in *erg9* and/or *coq1* might affect energy metabolism, we measured intracellular ATP concentration in wild-type and mutants. As shown in Fig. 3, the level of intracellular ATP in the *erg9* and *coq1* dual disruptant was lowest and that in wild type is highest in all strains, while the intracellular ATP level of the *erg9* disruptant was lower than that of the *coq1* disruptant. Since the fact that oxidative phosphorylation of the mitochondria is the main source of intracellular ATP supply and that a substantial proton gradient indicated by mitochondrial membrane potential is required for active oxidative phosphorylation, we further measured mitochondrial membrane potential in the strains. As shown in Fig. 4, the *erg9* disruptant, *coq1* disruptant, *erg9* and *coq1* dual disruptant had lower mitochondrial membrane potentials compared with the wild-type strain at 0 h. The membrane potential of all strains except the *erg9* and *coq1* dual disruptant decreased after 4 h, however, that of the *erg9* and *coq1* dual

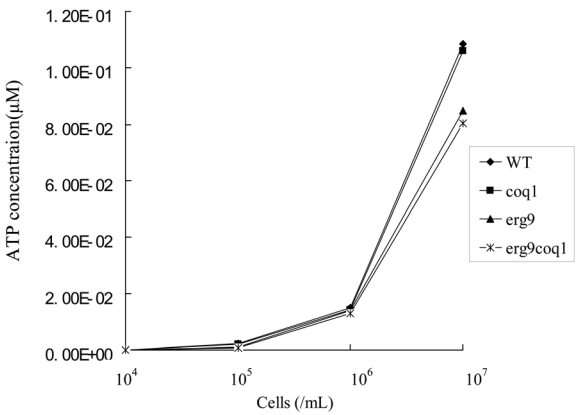

Fig. 3 Intracellular ATP content in *S. cerevisiae*. ATP levels represent the mean of three separate experiments. A linear correlation between ATP concentration and fungi cell numbers was detected in BY47439(WT), BY4743-Δ*erg9*(erg9), BY4743-Δ*coq1*(coq1), BY4743-Δ*erg9*-Δ*coq1*(erg9 coq1).

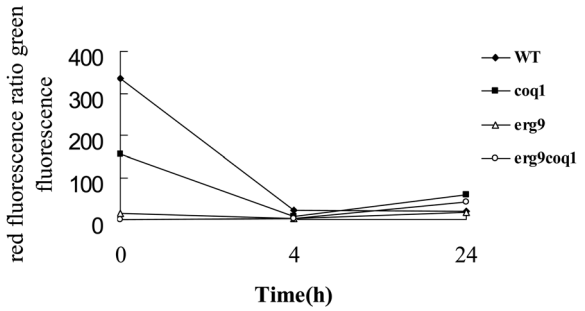

Fig. 4 Mitochondrial membrane potential was assessed by JC-1 red/green fluorescence ratio. Each sample was assayed in triplicate.

disruptant strain increased. Membrane potential of the wild-type strain continued to decrease after 24 h, however, that of the *erg9* disruptant, *coq1* disruptant, *erg9* and *coq1* dual disruptant increased. There is no significant difference in the new membrane potential balance between strains. These results suggest that a lower mitochondrial membrane potential resulting in a less efficient oxidative phosphorylation in the resistant strain may be the major cause of its lower ATP level and therefore change in its energy supply pathway from mitochondria to cytoplasm.

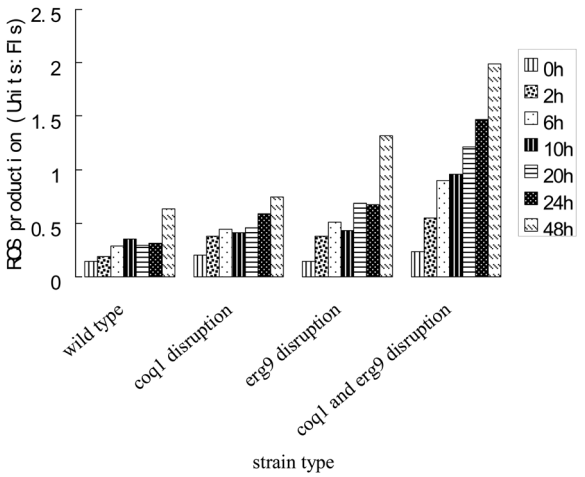

Fig. 5 Effects of *coq1* and *erg9* on intracellular ROS generation in the strains BY4743, BY4743-Δ*erg9*, BY4743-Δ*coq1*, BY4743-Δ*erg9*-Δ*coq1*. The level of endogenous ROS production was measured at the indicated time. Each datum point represents the mean for three independent experiments. Units of ROS production: fluorescence intensities, FIs.

Since intracellular oxygen radicals are mainly generated in mitochondria and are involved in the mechanisms of apoptosis in yeast, we examined endogenous ROS generation in the strains with the fluorescent dye DCFH-DA (Fig. 5). The alterations of ROS production over time are shown in Fig. 5. The highest level of intracellular ROS was observed in the *erg9* and *coq1* dual disruptant at each time-point measurement. The lack of *erg9* resulted in a further increase in ROS levels compared to that of *coq1*. ROS levels in all strains were significantly enhanced after 48 h, which could be explained by the lack of nutrients in the PBS medium resulting in stress within the cells.

3.4. Effect of *erg9* and *coq1* disruption on the sesquiterpene product diversity

To evaluate the effect of improved substrate availability on sesquiterpene production, we introduced into the above strains heterologous terpene synthase genes from plants. Plant sesquiterpene synthases, a subset of the terpene synthase superfamily, mostly are multi-product enzymes capable of synthesizing various structural terpenoids. The *TPS* genes from *M. grandiflora* have attracted attention because *M. grandiflora* possesses its evolutionary position as an ancestral or basal angiosperm. We chose one of the *M. grandiflora TPS* genes, which encoded sesquiterpene synthase catalyzing reactions in yielding multiple, chemically diverse reaction products.

Sesquiterpene product analysis by GC-MS of yeast strains transformed with pYES-Mg25 plasmid revealed the difference in the sesquiterpene profile strictly connected with the genetic background of the strain (Table 4, Fig. 6). Sesquiterpene products *in vivo* synthesized were identified by a combination of retention time and mass spectra in comparison with National Institute of Standards and Technology (NIST) library matches.[28]

The number and complexity of sesquiterpene products made it difficult to assess terpene productivity of the yeast strains, however, it may be interesting to open the way to additional improvement in diversity. Sesquiterpene products by the *S. cerevisiae* strains BY4743, BY4743-Δ*erg9*, BY4743-Δ*coq1*, and BY4743-Δ*erg9*-Δ*coq1* was compared. BY4743-Δ*erg9* was the best strain for the production of the most multiple sesquiterpenes, α-muurolol, α-bisabolol, and compound 4. BY4743 can produce only one sesquiterpene, globulol. BY4743-Δ*erg9*-Δ*coq1* can produce two sesquiterpenes, α-muurolol and α-bisabolol, however, BY4743-Δ*coq1* cannot be detected to produce any sesquiterpenes. This product profile contrasts with

Table 4 *In vivo* sesquiterpene products generated by β-cubebene synthase from *M. grandiflora*

				Host strains			
				BY4743	BY4743-Δ*erg9*	BY4743-Δ*coq1*	BY4743-Δ*erg9*-Δ*coq1*
Culture conditions	Medium			Sesquiterpene profile (number stands for peak shown in Fig. 6)			
With O_2	SG dropout medium			1	2,3,4	0	2,3
	SG dropout medium with additional metal ion	Divalent (M^{2+})	$MgSO_4$	3,5,6			
			$FeSO_4$	1,3,5			
			$MnCl_2$	3,5,6,7			
		Monovalent (M^{+})	KH_2PO_4	7			
Without O_2	SG dropout medium			1,3,5,8			

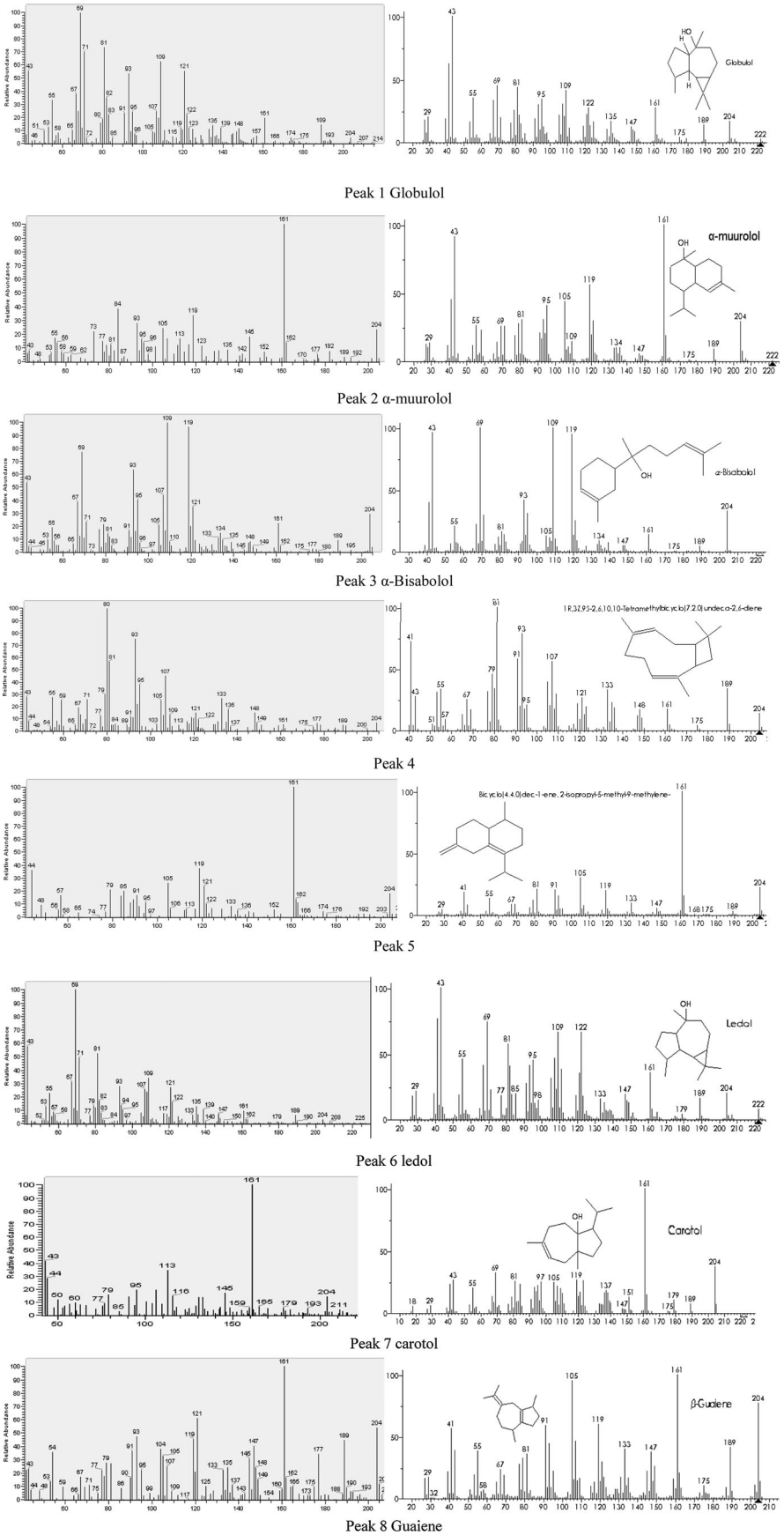

Fig. 6 Mass spectra for the identified sesquiterpenes with those in the NIST mass spectra library in Table 4. One peak number stands for individual compound detected in the induced strains harboring pYES-Mg25 (see Table 4).

the results obtained with the same enzyme *in vitro* assays from *E. coli* incubated with FPP.[17] Lee and Chappell (2008)[17] demonstrated that the dominant reaction products generated by Mg25 were β-cubebene, α-muurolene, δ-cadinol, δ-elemene, τ-muurolene, and β-elemene.

Cofactors are often required for biochemical transformations mediated by metabolic enzymes by metabolic enzymes. It is important to consider the availability of necessary cofactors as well as the balance of electron-mediating cofactors. Formation of terpenoids from their respective 10-, 15-, or

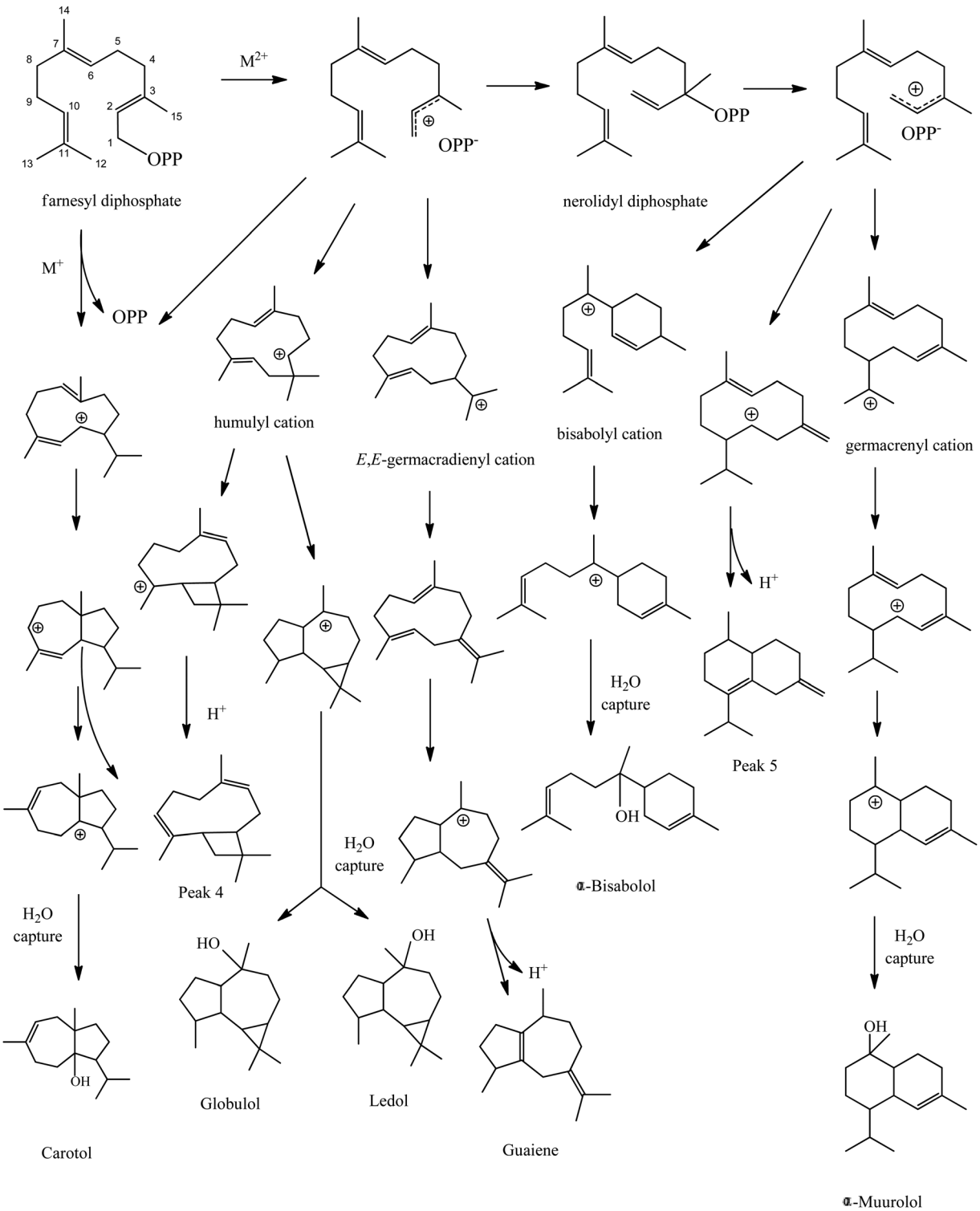

Fig. 7 Proposed reaction mechanisms rationalizing the sesquiterpene reaction products generated by β-cubebene synthase from *M. grandiflora*.

20-carbon atom prenyl diphosphate precursors is initiated by divalent (M^{2+}) metal ion-assisted electrophilic attack. In addition to M^{2+}, monovalent cations (M^{+}) have also been shown to be essential for the activity of certain terpene synthases most likely by facilitating substrate binding or catalysis. We also investigated the effect of different metal ions on sesquiterpene production outcome. The results showed that the addition of metal ions as cofactors can increase the structural diversity of sesquiterpene production. Wild type strains only can produce globulol under no additional metal ion medium, but can produce α-bisabolol, compound 5, and ledol with Mg^{2+} initiation, and globulol, α-bisabolol and compound 5 with Fe^{2+} initiation. The most diversity in sesquiterpene production came from the Mn^{2+} initiation to generate α-bisabolol, compound 5, ledol and carotol. Compared with divalent metal ions, the role of monovalent cations is much weaker in the synthesis of sesquiterpenes, which produced one single structure, carotol.

S. cerevisiae is able to grow both aerobically and anaerobically. To evaluate the yeast's performance to stress tolerance from respiratory metabolism to fermentation, we compared the production of sesquiterpenes under two conditions. Under anoxic conditions, wild type strains have the ability to produce more structurally diverse sesquiterpenes compared to oxic conditions. The reaction products were globulol, α-bisabolol, compound 5 and guaiene without oxygen.

The potential reaction mechanism of Mg25 begins with the ionization of farnesyl diphosphate which in some isozymes isomerizes to the nerolidyl cation (Fig. 7). The multiple reaction products shown may result from farnesyl diphosphate or nerolidyl diphosphate, through a series of hydride shifts, ring closures, deprotonations, and a hydroxide capture (Fig. 7).

3.5. Effect of *erg9* and *coq1* disruption on the diterpene production

The copalyl diphosphate synthases (CPS) and the normal CPP kaurene synthase-like (KSL) from *S. miltiorrhiza* have previously been reported to catalyze GGPP into diterpene hydrocarbon. We also tried to gain additional insights into the mechanism for diterpene production. The *S. miltiorrhiza* CPS cDNA and KSL cDNA were inserted into pESC-Ura yeast expression vector, and the constructed pESC-SmKSL-SmCPS plasmid was transformed into four types of yeast cell hosts. It was reported that SmCPS belongs to class II (CPS-type) diterpene cyclases, and catalyzed an initial carbon–carbon double-bond protonation-initiated reaction typically from GGPP to labdadienyl/copalyl diphosphate (CPP). On the other hand, SmKSL as a class I (KS-type) diterpene synthase, initiates the subsequent cyclization of CPP by an elimination of the diphosphate group in CPP and/or rearrangement of the carbon skeleton of CPP to form diterpene skeleton-miltiradiene (**10**).

Because there is no mass spectrum of miltiradiene in the National Institute of Standards and Technology (NIST) library, we created the diterpene profile in *S. miltiorrhiza* hairy root. We firstly confirmed miltiradiene really existed in fresh plant hairy root, whose mass spectrum is shown to be identical with that of the enzymatic product previously reported by Gao *et al.*[18] The result can support the hypothesis that miltiradiene is a precursor leading to tanshinone biosynthesis. It was observed that *in vivo* synthesis of plant diterpenes by four strains harboring plasmid pESC-SmKSL-SmCPS by GC-MS, only thunbergol (**9**) can be detected by wild type BY4743 and BY4743-Δ*erg9* without any additional metal ion, and the yield of thunbergol in BY4743-Δ*erg9* was higher than that in WT strains. Under the same conditions, we did not detect any diterpene in BY4743-Δ*erg9*-Δ*coq1* and BY4743-Δ*coq1*, which was probably below the level of detection. Without additional metal ions, miltiradiene was not detected as expected.

However, the BY4743 harboring plasmid pESC-SmKSL-SmCPS can generate thunbergol and miltiradiene after adding Mg^{2+}. With addition of Mn^{2+}, they still produced miltiradiene, but no thunbergol. And no diterpenes were detected with Fe^{2+} and monovalent initiation (Table 5, Fig. 8). These results are proof that the inability of M^{+} to direct catalysis, unlike divalent metal ions (*e.g.* M^{2+} in TPS), results from insufficient charge density, due to the spread of a single charge over a large volume.[29] The tight *in vivo* regulation of M^{+} levels[28] also means that the enzyme active site would always be charged with M^{+}, and M^{+} would not be a physiologically relevant regulator of enzyme activity. The proposed biochemical mechanism of diterpene synthase is depicted Fig. 9.

3.6. Improved substrate availability enhances terpene diversity and production but does not overcome the negative effects of *COQ1* deletion

From the intermediates levels through the MVA pathway, we can see enhancement of GPP, FPP, and GGPP by *erg9* knockout. BY4743-Δ*erg9* engineered with TPS was able to produce more diversity and yields of terpene products than the parental strain with TPS alone. In contrast, a strain with TPS and lacking *erg9* and *coq1* did not improve terpene production, even though there was improvement in substrate availability. In combination with the energy and redox status, deletion of *coq1* may result in some imbalance which in many cases blocked the desired product generation.

Table 5 *In vivo* diterpene products generated by coexpression of CPS and KSL from *S. miltiorrhiza*. The peaks 9 and 10 are shown in Fig. 8

		Divalent (M^{2+}) metal ion			Monovalent (M^{+}) metal ion
Host strains	No additional metal ion	$MgSO_4$	$FeSO_4$	$MnCl_2$	KH_2PO_4
BY4743	Peak 9 (thunbergol)	Peak 9,10 (miltiradiene)	0	Peak 10	0
BY4743-Δ*erg9*	Peak 9 (thunbergol)				
BY4743-Δ*coq1*	0				
BY4743-Δ*erg9*-Δ*coq1*	0				

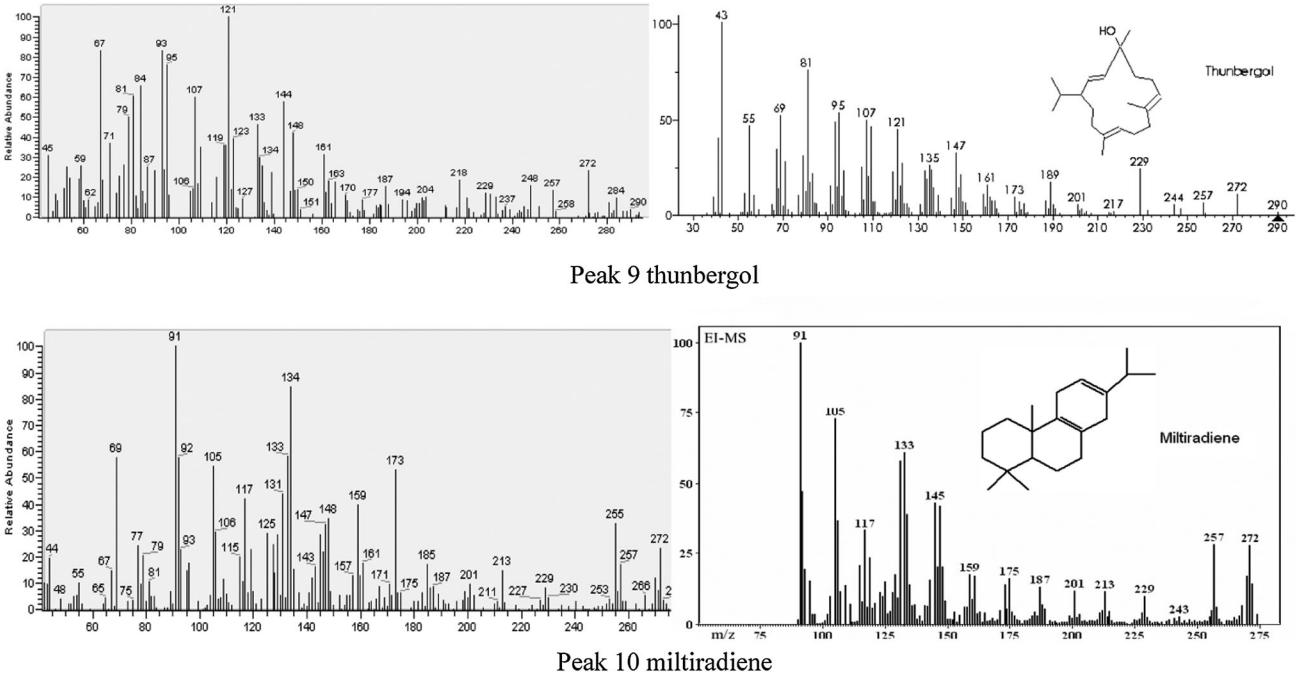

Fig. 8 Mass spectra for the identified diterpenes with those in the NIST mass spectra library and ref. 18 in Table 5.

4. Discussion

In this study, we investigated the effects of deregulating the mevalonate pathway in the yeast *S. cerevisiae* on the isoprenoids biosynthesis. Physiological analysis would help us illuminate the effects of perturbation in pathways of interest, as well as unbiased characterizations of microbial stress responses as a whole. The effects of the manipulations on the endogenous pathway were also studied by analyzing chemical diversity and yield of terpene production in the engineered strains.

Recent advances in metabolic engineering represent a paradigm shift from focusing only on the product forming step, and instead understanding the pathway in the context of the entire cell. Based on our previous work,[27] *coq1* and *erg9* can be targets for redirecting sterol precursors to the phosphorylated isoprenoid pathway, which may be effective for terpenoids production. Also, targeting of terpenoid production pathway components to the mitochondria significantly increased yields.[30] COQ1 belongs to mitochondrial proteins, which could shed light on the mechanism of terpenoid biosynthesis in the metabolic engineering field.

Mechanisms for *in vivo* assessment have also been described including the use of knockout mutations and RNA suppression technologies and the observed loss of a particular metabolite profile.[31,32] To determine the role of *erg9* and *coq1* in isoprenoids biosynthesis in *S. cerevisiae*, we generated *coq1* disruptant, *erg9* disruptant, *coq1* and *erg9* dual disruptant with a PCR-mediated gene knockout.

In order to understand how the *in vivo* flux through the pathway is regulated, we conducted metabolic target analysis by GC-SIM-MS coupled with chemometrics. The gene-to-metabolite correlation can be revealed by analyses of intracellular metabolite levels in response to gene knockout. We observed there is likely to be a more close relationship with the level of *erg9* and phosphorylated isoprenoid through the pathway, whereas there seems to be an inverse correlation between the levels of *coq1* and sterols.[27]

Because *coq1* and *erg9* contribute many different functions to cellular physiology, it is of interest to ask what kinds of changes might be tolerated by cells without affecting this fundamental physiological role. The growth rate of the resultant mutant was lower than that for unmutated *S. cerevisiae*, however, the mutant strains can still keep growing and reproduce. In order to understand metabolic changes that underlie the unique physiology of the mutant strain, we used physiological characterization to decipher possible metabolism alterations.

Physiological analysis revealed slower cell growth, greater energy-dependent efflux activity of membrane transporters, lower intracellular ATP level and mitochondrial membrane potential, more endogenous reactive oxygen species generation in response to gene disruption. Mitochondria provide a majority of cellular ATP, and a substantial mitochondrial membrane potential is required for mitochondrial ATP synthesis. The measurement of ATP content and the mitochondrial membrane potential revealed lower intracellular ATP levels and even lower mitochondrial membrane potential in the mutant strain, suggesting a deficiency in oxidative phosphorylation and lower mitochondria-based source of ATP supply. Both *coq1* and *erg9* are energy-metabolism-related proteins.

Squalene synthase (SQS), encoded by *erg9*, catalyzes the first committed step of ergosterol synthesis and plays a key role in determining the flux through the FPP branch point. Ergosterol regulates the fluidity of the yeast cell membrane and has been found to be essential for yeast growth. The repression of *erg9*

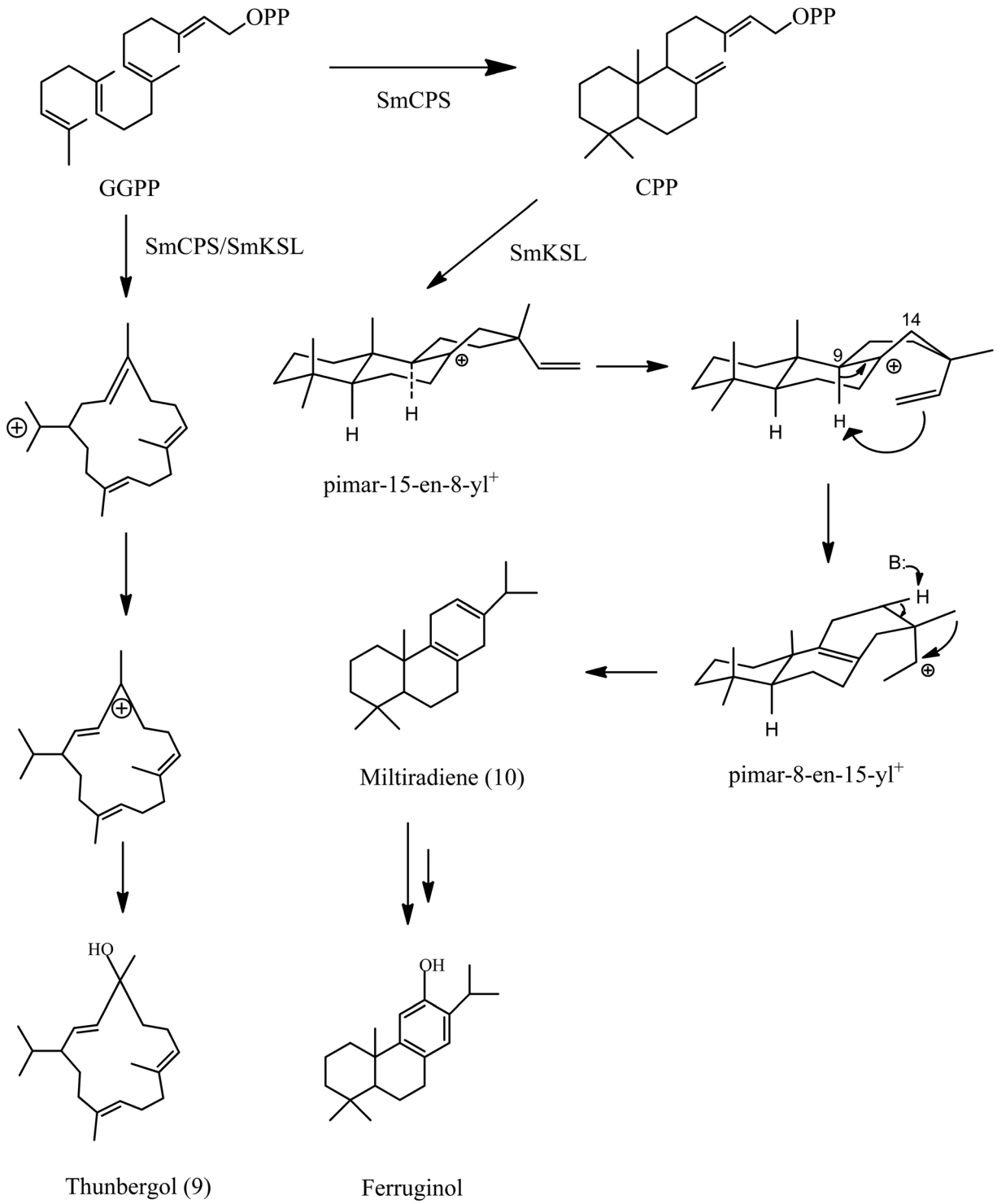

Fig. 9 Proposed reaction mechanisms rationalizing the diterpene reaction products generated by coexpression of SmCPS and SmKSL.

led to lower specific growth rates compared to the wild type strain and reduced the ergosterol content in the yeast strains. This was confirmed by metabolic targeted analysis. The yeast *COQ1* gene encodes a hexaprenyl diphosphate synthase[33] responsible for determining the tail length of ubiquinone (coenzyme Q).[34] Coenzyme Q plays an important role in energy metabolism, and energy balance also plays an important role in the metabolic regulation. Controlling respiration and redox through genetic modifications may serve as a promising alternative for secondary metabolic products. Under the deletion of the *erg9* or/and *coq1* conditions, the mitochondrial respiratory chain is blocked when there are no other electron acceptors.

Thus, ATP used for the cell growth is less generated, which was further confirmed by growth determination. We found that the growth of mutants (*coq1* disruptant, *erg9* disruptant, *erg9* and *coq1* dual disruptant) was slower than wild-type cells. We speculate that the decrease of energy metabolism might exist in the mutants, which contributed to the slower growth rate.

Since the primary source of endogenous ROS, normal byproducts of energy production in respiring cells, is leakage of electrons from the mitochondrial respiratory chain,[35,36] and the increase of intracellular ROS production is one of the factors responding to oxidative stress, we speculated that excess ROS are generated in mutant strains due to mitochondrial respiration deficiency which might result from *erg9* or/and *coq1* knockout. With the glucose-induced R6G efflux assay, we further demonstrated that efflux of R6G in yeast is energy-dependent, the gene deficiency reduced the energy metabolism, leading to a decrease in the activity of the energy-dependent efflux pump.

Microorganisms coordinately adapt their respiration and metabolism to environmental changes, and metabolic profiles of the cells are intrinsically different under different energy conditions.[37,38] To further evaluate substrate availability, cofactor and mitochondrial function in the regulation of isoprenoids synthesis, heterologous terpene synthases were introduced into *S. cerevisiae*, including the wild-type and mutant strains. The knockouts of *erg9* and *coq1* genes significantly changed intracellular metabolites levels of the MVA pathway, which are usually used as substrates for terpene production. We focus on the sesquiterpenes diversity and diterpenes production; β-cubebene synthase from *Magnolia grandiflora* is a typical plant sequiterpene synthase well-documented for its capacity to generate multiple reaction productions.[17] In contrast, copalyl diphosphate synthases (CPS) and kaurene synthase-like (KSL) from *Salvia miltiorrhiza* Bunge were reported to be quite specific in diterpene production, of which one novel diterpene named as miltiradiene was a single dominant product.[18] The results showed that β-cubebene synthase was clearly capable of catalyzing the conversion of FPP into multiple sesquiterpenes. Since most of the FPP is used for the biosynthesis of sterols, minimizing the flux of FPP towards sterols should enhance available FPP for other enzymes of the FPP branchpoint including sesquiterpene synthases. So it is obvious that BY4743-Δ*erg9* produced the most diverse sesquiterpene skeletons among four strains. But BY4743-Δ*erg9*-Δ*coq1* did not show more capacity in terpenoid diversity and yield, furthermore with BY4743-Δ*coq1* terpenoid production cannot be detected. We speculated that the presence of *coq1* is vital for terpenoid synthesis *in vivo*.

It is considered that the product spectrum represents the final outcome of the intracellular metabolic regulation at many different levels. Genetic manipulation changed substrate levels, the intracellular redox state and, therefore, changed the fraction of the metabolic end products. Under anaerobic and aerobic conditions, the terpene profiles in yeast are intrinsically different. With sufficient oxygen supply, cells produce ATP through respiration and grow rapidly, but a lot of carbon atoms are lost in the form of CO_2. Under anaerobic conditions, cells convert most of the carbon source to primary and secondary metabolites. This is in accordance with our observation that wild type strains produced more structurally diverse sesquiterpenes without oxygen. The metal ion, divalent or monovalent, plays an important role in the binding of the substrate to the enzyme by forming ionic bridges between the negatively charged pyrophosphate group of the substrate FPP and negatively charged residues in the active site. Different metal ions showed different enzyme efficiency, the turnover in the presence of monovalent metal ions is lower compared to in the presence of divalent metal ions, and Mn^{2+} seems to be better than Mg^{2+}. However, the sequiterpene composition in the recombinant yeasts is much different from an analysis of sequiterpenes found in fresh Magnolia leaves. It could be the biosynthesis of terpenoids in plants is ingeniously regulated at the subcellular level. For example, whereas the primary carbon skeletons of monoterpenes and diterpenes are produced in plastids, the backbones of sesquiterpenes and triterpenes are produced in the cytosol.[39,40] Further enzymatic modifications to these backbones may also occur in different cell compartments such as the endoplasmic reticulum, where terpene backbones are hydroxylated. Mitochondria also participate in isoprenoid biosynthesis. The yeast system has many differences compared to the original plant host, which could explain why the sequiterpene profile is different. The observation in diterpene production is similar to sesquiterpene production, which could be probably due to slight differences existing in the terpene synthase function. Diterpene synthase usually produces one single dominant product, however, sequiterpene synthase, β-cubebene synthase, is multifunctional. The major product of *S. miltiorrhiza* diterpene synthase is miltiradiene, and a byproduct could be thunbergol.

All those actions are related to the mitochondrial function. Mitochondria carry out specialized functions; compartmentalized, yet integrated into the metabolic and signaling processes of the cell. The limiting nature of chemical complexity for the overall cell has been addressed related to the energy barrier. The global cellular energy status has a shift in the absence of genes, or addition of metal ions, further impacting on the profile of heterologous sesquiterpenes and diterpenes. When a heterologous terpenoid biosynthetic pathway was redirected to the mitochondria compartment, it dramatically increased terpene accumulation probably due to added access to a cofactor, precursor and energy supply. We speculated that the activation of mitochondrial energy metabolism could improve the metabolic flux rates, further leading to an enhancement in the target production. To further confirm our conclusion about the relationship between isoprenoid biosynthesis and mitochondrial function, future research will extend the candidates of other mitochondrial enzymes dependent of MVA pathway products such as the farnesyl group of heme A, the prostetic group of cytochrome *c* oxidase.

A multitude of small but crucial contributions to the generation of terpenoid biosynthesis are made by many factors. It is possible to combine the metabolic engineering approaches, byproduct elimination, precursor enrichment, cofactor optimization

and enhancement of metabolic flux rates to increase the desired compounds production. The redirection of biosynthesis compartments provides us a new insight into the regulation of metabolic engineering.

Conflicts of interest

The authors declare that they have no conflict of interest.

Acknowledgements

This research was funded by Shanghai Science and Technology Committee (No. 054319936) to BBH and the National Natural Science Foundation of China (No. 20702062) to BBH.

References

1 J. Gershenzon and N. Dudareva, *Nat. Chem. Biol.*, 2007, **3**, 408–414.
2 P. Lindberg, S. Park and A. Melis, *Metab. Eng.*, 2010, **12**, 70–79.
3 S. Atsumi and J. C. Liao, *Curr. Opin. Biotechnol.*, 2008, **19**, 414–419.
4 J. Bohlmann and C. I. Keeling, *Plant J.*, 2008, **54**, 656–669.
5 K. E. Tyo, H. S. Alper and G. N. Stephanopoulos, *Trends Biotechnol.*, 2007, **25**, 132–137.
6 L. Kizer, D. J. Pitera, B. F. Pfleger and J. D. Keasling, *Appl. Environ. Microbiol.*, 2008, **74**, 3229–3241.
7 K. Hiller, C. Metallo and G. Stephanopoulos, *Curr. Pharm. Biotechnol.*, 2011, **12**, 1075–1086.
8 R. Rios-Estepa, G. W. Turner, J. M. Lee, R. B. Croteau and B. M. Lange, *Proc. Natl. Acad. Sci. U. S. A.*, 2008, **105**, 2818–2823.
9 G. Jia, G. N. Stephanopoulos and R. Gunawan, *Bioinformatics*, 2011, **27**, 1964–1970.
10 E. Leonard, P. K. Ajikumar, K. Thayer, W. H. Xiao, J. D. Mo, B. Tidor, G. Stephanopoulos and K. L. Prather, *Proc. Natl. Acad. Sci. U. S. A.*, 2010, **107**, 13654–13659.
11 L. Albertsen, Y. Chen, L. S. Bach, S. Rattleff, J. Maury, S. Brix, J. Nielsen and U. H. Mortensen, *Appl. Environ. Microbiol.*, 2011, **77**, 1033–1040.
12 K. E. Tyo, E. Nevoigt and G. Stephanopoulos, *Methods Enzymol.*, 2011, **497**, 135–155.
13 J. D. Keasling, *ACS Chem. Biol.*, 2008, **3**, 64–76.
14 D. Endy, *Nature*, 2005, **438**, 449–453.
15 J. C. Anderson, J. E. Dueber, M. Leguia, G. C. Wu, J. A. Goler, A. P. Arkin and J. D. Keasling, *J. Biol. Eng.*, 2010, **4**, 1.
16 L. Martin, A. Che and D. Endy, *PLoS One*, 2009, **4**, e7569.
17 S. Lee and J. Chappell, *Plant Physiol.*, 2008, **147**, 1017–1033.
18 W. Gao, M. L. Hillwig, L. Huang, G. Cui, X. Wang, J. Kong, B. Yang and R. J. Peters, *Org. Lett.*, 2009, **11**, 5170–5173.
19 M. D. Rose, F. Winston and P. Hieter, *Methods in Yeast Genetics*, Cold Spring Harbor Laboratory Press, New York, 1990.
20 F. Sherman, G. R. Fink and J. B. Hicks, *Methods in Yeast Genetics*, Cold Spring Harbor Laboratory Press, New York, 1986.
21 D. K. Ro, E. M. Paradise, M. Ouellet, K. J. Fisher, K. L. Newman, J. M. Ndungu, K. A. Ho, R. A. Eachus, T. S. Ham, J. Kirby, M. C. Chang, S. T. Withers, Y. Shiba, R. Sarpong and J. D. Keasling, *Nature*, 2006, **440**, 940–943.
22 J. D. Boeke, F. LaCroute and G. R. Fink, *Mol. Gen. Genet.*, 1984, **197**, 345–346.
23 H. Ito, Y. Fukuda, K. Murata and A. Kimura, *J. Bacteriol.*, 1983, **153**, 163–168.
24 J. Sambrook, E. F. Fritsch and T. Maniatis, *Molecular cloning: a laboratory manual*, Cold Spring Harbor Laboratory Press, New York, 1989.
25 S. Salvioli, A. Ardizzoni, C. Franceschi and A. Cossarizza, *FEBS Lett.*, 1997, **411**, 77–82.
26 K. Grabinska and G. Palamarczyk, *FEMS Yeast Res.*, 2002, **2**, 259–265.
27 B. Huang, H. Zeng, L. Dong, Y. Li, L. Sun, Z. Zhu, Y. Chai and W. Chen, *Metabolomics*, 2011, **7**, 134–146.
28 D. M. Martin, J. Faldt and J. Bohlmann, *Plant Physiol.*, 2004, **135**, 1908–1927.
29 M. J. Page and E. Di Cera, *Physiol. Rev.*, 2006, **86**, 1049–1092.
30 M. Farhi, E. Marhevka, T. Masci, E. Marcos, Y. Eyal, M. Ovadis, H. Abeliovich and A. Vainstein, *Metab. Eng.*, 2011, **13**, 474–481.
31 D. Tholl, F. Chen, J. Petri, J. Gershenzon and E. Pichersky, *Plant J.*, 2005, **42**, 757–771.
32 E. Wang and G. J. Wagner, *Planta*, 2003, **216**, 686–691.
33 M. N. Ashby and P. A. Edwards, *J. Biol. Chem.*, 1990, **265**, 13157–13164.
34 K. Okada, K. Suzuki, Y. Kamiya, X. Zhu, S. Fujisaki, Y. Nishimura, T. Nishino, T. Nakagawa, M. Kawamukai and H. Matsuda, *Biochim. Biophys. Acta*, 1996, **1302**, 217–223.
35 K. Staniek, L. Gille, A. V. Kozlov and H. Nohl, *Free Radical Res.*, 2002, **36**, 381–387.
36 D. L. Danley, A. E. Hilger and C. A. Winkel, *Infect. Immun.*, 1983, **40**, 97–102.
37 A. Böck and G. Sawers, in *Escherichia coli and Salmonella: Cellular and Molecular Biology*, ed. F. C. Neidhardt, R. Curtiss, J. L. Ingraham, E. C. C. Lin, K. B. Low, B. Magasanik, W. S. Reznikoff, M. Riley, M. Schaechter and H. E. Umbarger, ASM Press, Washington, DC, 1996, pp. 262–282.
38 A. S. Lynch and E. C. C. Lin, in *Escherichia coli and Salmonella: Cellular and Molecular Biology*, ed. F. C. Neidhardt, R. Curtiss, J. L. Ingraham, E. C. C. Lin, K. B. Low, B. Magasanik, W. S. Reznikoff, M. Riley, M. Schaechter and H. E. Umbarger, ASM Press, Washington, DC, 1996, pp. 1526–1538.
39 S. Wu, M. Schalk, A. Clark, R. B. Miles, R. Coates and J. Chappell, *Nat. Biotechnol.*, 2006, **24**, 1441–1447.
40 A. Aharoni, M. A. Jongsma and H. J. Bouwmeester, *Trends Plant Sci.*, 2005, **10**, 594–602.

